Density Functional Theory Analysis of Dichloromethane and Hydrogen Interaction with Pd Clusters: First Step to Simulate Catalytic Hydrodechlorination

ARTICLE *in* THE JOURNAL OF PHYSICAL CHEMISTRY C · JUNE 2011

Impact Factor: 4.77 · DOI: 10.1021/jp200329j

6 AUTHORS, INCLUDING:

Salama Omar
Universidad Autónoma de Madrid
15 PUBLICATIONS **132** CITATIONS
SEE PROFILE

Luisa M. Gómez-Sainero
Universidad Autónoma de Madrid
26 PUBLICATIONS **341** CITATIONS
SEE PROFILE

Maria Ariadna Álvarez-Montero
Universidad Autónoma de Madrid
12 PUBLICATIONS **97** CITATIONS
SEE PROFILE

Maria Martin-Martinez
Instituto Politécnico de Bragança
11 PUBLICATIONS **76** CITATIONS
SEE PROFILE

THE JOURNAL OF PHYSICAL CHEMISTRY C

ARTICLE

pubs.acs.org/JPCC

Density Functional Theory Analysis of Dichloromethane and Hydrogen Interaction with Pd Clusters: First Step to Simulate Catalytic Hydrodechlorination

Salama Omar, Jose Palomar,* Luisa M. Gómez-Sainero, Maria A. Álvarez-Montero, Maria Martin-Martinez, and Juan J. Rodriguez

Departamento de Química Física Aplicada, Sección de Ingeniería Química, Facultad de Ciencias, Universidad Autónoma de Madrid, 28049 Spain

ABSTRACT: A density functional theory (DFT) analysis has been conducted for the gas-phase hydrodechlorination (HDC) of dichloromethane (DCM) with palladium catalyst to achieve a better knowledge of the reaction mechanism involved in the HDC process, which constitutes an emerging technology for the treatment of organochlorinated contaminants. The computational study included the effect of size, oxidation state, and spin configuration of Pd cluster on the adsorption of H_2 and DCM reactants on the catalyst surface. Calculations described the activation of H_2 by Pd clusters through a dissociative adsorption with low enthalpy values. In addition, partially and fully dissociated DCM intermediates on Pd surface were predicted by DFT calculations. Remarkably, the dissociative adsorption of DCM on Pd active sites occurs via the scission of C−Cl bonds, promoted by the formation of C−Pd linkages, implying high adsorption enthalpy. The computational results showed that DCM can be also molecularly adsorbed on both zerovalent and electrodeficient Pd species. However, the nondissociative adsorption of DCM over electrodeficient Pd cluster is remarkably favored in energy, with adsorption enthalpies (∼−50 kcal/mol) corresponding to chemisorption. Current theoretical evidence explained the deactivation of Pd/AC catalyst as a consequence of the selective poisoning of electrodeficient Pd active centers by chlorinated hydrocarbons, in good agreement with our previous experimental findings.

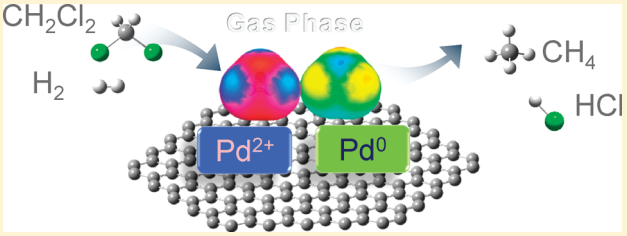

1. INTRODUCTION

Environmental catalysis is a field of growing interest, due to the increasingly stringent regulations for pollutant emission. To reduce the environmental impact of the industrial processes, it is necessary to develop more active, selective, and stable catalysts.[1] A fundamental premise for the rational and competitive design of new catalysts is to have a good knowledge on the factors that determine their behavior. A great effort in the characterization of materials has been afforded to understand why they behave as good catalyst in a particular reaction. In this sense, the simulation of catalytic phenomena by rigorous quantum-chemical methods can be exploited for the design of materials with favorable catalytic properties for a given reaction.

This work reports an attempt to investigate, by simulation with the density functional theory (DFT), the hydrodechlorination (HDC) of organochlorinated compounds in gas phase with palladium (Pd) catalysts supported on activated carbon (AC), which has been experimentally studied by our group in previous works.[2−6] The release of organic chlorinated compounds, such as chloroform, carbon tetrachloride, tetrachloroethylene, and dichloromethane (DCM), into the environment is of considerable concern.[7] In fact, emissions of organochlorinated pollutants have been progressively restricted in the last years by environmental regulations because of their toxicity, carcinogenic character, and potential contribution to the destruction of the ozone layer.[8−10] This leads to the need of developing effective treatment techniques that are environmentally friendly. Catalytic HDC represents one of the most promising emerging technologies with potential economic and environmental advantages with respect to incineration for treating waste gases containing organochlorinated compounds. It operates under moderate conditions, and the reaction products are much less hazardous. Among the used metals, Pd is usually considered to be one of the best catalysts for that process because of its high activity and selectivity toward nonchlorinated products.[2−6,11,12] Pd is less prone to deactivation by chlorine than other transition metals.[13] Electrodeficient palladium, Pd^{2+}, has been reported to improve the activity of Pd catalysts in HDC reactions,[3,14−18] and, in some cases, the adsorption of the chlorinated reactant has been proposed to occur mainly on Pd^{2+}.[14,19] The metal particle size has a significant influence on the performance of Pd catalysts regarding activity and selectivity.[19−24] The support also plays a significant role in the performance of Pd catalysts. ACs are effective supports for HDC reactions because of both physical and chemical properties.[25] High dispersion of metallic particles can be achieved using ACs with high surface areas and the appropriate surface composition.[5,19,26] Pd/carbon catalysts prepared from

Received: January 12, 2011
Revised: May 9, 2011
Published: June 30, 2011

aqueous solutions have been reported to be resistant to metal sintering and HCl poisoning,[2,3,19] in contrast with those using SiO_2, Al_2O_3, MgO, TiO_2, ZrO_2, and AlF_3 supports.[27] In previous works of our research group,[2−5] the gas-phase HDC of trichloromethane (TCM), DCM, and monochloromethane (MCM) in the temperature range of 150−250 °C with Pd/AC catalysts was investigated. These catalysts showed high activity and selectivity to nonchlorinated products, although an important deactivation was observed. The active centers were constituted by the association of Pd^0 and Pd^{2+}, where the latter species was formed by interaction of metal particles with the carbon surface. The catalysts were found highly resistant to metal sintering, HCl poisoning, and coke formation, the results suggesting deactivation to occur through metal poisoning of active centers by chlorine-containing reactants, intermediates, or reaction products. Four issues arise from the above-mentioned experimental evidence that we wish to address now by simulation: (i) a better knowledge of the reaction mechanisms on Pd active sites involved in HDC process toward the formation of different chlorinated and nonchlorinated products; (ii) why the catalyst activity follows the same order as the chlorine content of the pollutant (TCM > DCM > MCM); (iii) why the catalyst is deactivated and why the deactivation is higher in the case of DCM than with TCM or MCM; and (iv) what is the role of the neutral (Pd^0) and electrodeficient (Pd^{2+}) active species present in the catalyst on its behavior in terms of activity, selectivity, and stability.

During the past 10 years, the number of theoretical works on the description of the reactions that occur in surfaces has significantly grown.[28] Advances in density functional methods have determined that it is now computationally possible to describe catalytic reactions on surfaces with sufficient detail and precision to explain the experimental evidence.[29,30] Complementing the experimental studies, simulation using reliable quantum chemical methods can provide information on an atomic or molecular level on the effect of the interactions taking place in the active sites of the catalyst, thereby contributing to the interpretation of the mechanisms, barriers of energy and intermediate species involved in the reaction as well as on the effect of the support-active species interactions on the catalyst performance.[31,32] The basic idea for the catalyst simulation is that chemisorption and reactivity are local phenomena, primarily affected by the surface structure nearest the active sites. As a result, one can use discrete atomic models to describe the components involved in the reaction and the region surrounding the active site. Regarding the simulation of Pd catalysts, the literature contains a number of recent theoretical works on the application of quantum chemical methods to these systems, focused on:

(i) The geometry and energy of Pd cluster depending of its size, oxidation state and spin configuration.[33] Palladium clusters have been simulated by a wide range of methods, covering from semiempirical[34] to the most complex post-SCF as well as DFT.[33] Recently, palladium clusters with larger nuclearity were also studied by molecular dynamics.[35]

(ii) The phenomenon of dissociative adsorption of hydrogen on Pd surfaces,[36] including adsorption of multiple molecules.[37−39] The activation of H_2 by Pd clusters has been computationally investigated depending on the size of the cluster[40] and the spin multiplicity as triplet or singlet state.[38,41,42] In these studies, the active species were described by means of models including one to seven atoms of Pd. The results showed that increasing the number (n) of Pd atoms implied higher Pd−Pd bond energies until $n = 6$, size from which energy stabilization remained nearly constant. In addition, it was shown that dissociative adsorption occurred on Pd_n cluster from $n = 3$, reaching a constant energy stabilization beyond $n = 6$. Concerning the influence of the ground spin state, a multiplicity lowering from the triplet to the singlet upon hydrogen fragmentation was reported for the Pd_4 system.[38,41,42]

(iii) The interactions of the Pd particles with AC used as support.[43] It was found that Pd atoms interact more effectively with the defects (unsaturated carbons) on the surface of AC than with graphitic layers. Also, it was found that the Pd clusters tend to form small pseudospherical particles, with structures determined by triangular faces, which interact effectively with accessible sites (unsaturated carbon atoms) of AC, justifying the high dispersion of Pd on the surface of this support and the preference for being selectively adsorbed in narrow pores.[44] More recent DFT studies on catalytic properties of palladium cluster supported on carbon nanotubes and surfaces analyzed the adsorption, fragmentation, and diffusion of hydrogen.[45−48]

(iv) The reactivity of short-chain hydrocarbons on Pd catalysts, considering reactants, intermediates, and products in the study of dehydrogenation of organic compounds.[49] Here the theoretical analysis sought to identify the elementary steps involved in the reaction mechanism, allowing the evaluation of the energy barriers by quantum-chemical calculations to further determine the reaction rate constants through statistical thermodynamic calculations. Other studies[50] have shown that the insertion of CH_x species on Pd clusters is favored energetically by increasing the number of Pd atoms.

(v) Interactions of other ligands with the Pd metal core. A series of works have analyzed the interactions of CO,[51−53] NO,[54] S,[55] Cl,[55] and O_2,[56] and methanol,[57] acetic acid,[58] acetate, and thiophene.[59]

Nevertheless, theoretical studies involving complex catalytic processes with Pd catalysts are scarce in the literature.[38−40] To the best of our knowledge, only one experimental kinetic and theoretical analysis of HDC of $CH_{4-x}Cl_x$ ($x = 1−4$) compounds on palladium has been reported,[63] DFT calculations were carried out to calculate transition states and to estimate the activation energies for the dissociation of the first C−Cl bond of chlorinated methane by using planar clusters of Pd atoms, obtaining a good agreement with the values extracted from kinetic modeling. The reaction mechanism of dechlorination of carbon tetrachloride,[64] 1,2-dichloroethane,[65] and chloroethenes[66] on different metals (Pt, Cu−Pt, and iron, respectively) has been analyzed by DFT calculations. In current work, a comprehensive theoretical study of the HDC of chlorinated organic compounds (DCM, TCM, and MCM) using palladium-based catalysts will be conducted to describe the interactions between the chemical species involved in the catalytic process using quantum chemical methods in the DFT framework. We begin with the computational analysis of the interaction between DCM and H_2 reactants and Pd catalytic surface, considering simultaneously the influence of size, oxidation state, and spin configuration of Pd cluster on adsorption phenomena and the formation of intermediate

species involved in the HDC reactions. In future works, the transition states that can reach the different products will be considered in the computational study to evaluate the energy barriers and possible reaction mechanisms and kinetics determining the different activity and selectivity shown by the catalyst.

2. COMPUTATIONAL METHODS

All computational studies were performed with the Gaussian 03[67] series of programs with density functional methods, as implemented in the computational package. The transition-metal clusters present a great number of electrons, which reorganize deeply the atomic electron density, so we have simulated palladium clusters using the DFT. The B3LYP functional combines the Becke three-parameter nonlocal hybrid exchange potential[68] and the nonlocal correlation functional of Lee, Yang, and Parr.[69] The chemical inert core orbitals of palladium clusters were described with the effective core potentials of Hay and Wadt,[70,71] which include relativistic effects on valence electrons, whereas the external orbitals were represented with a double-ζ basis set[72] using Dunning/Huzinaga full double-ζ basis set (Lanl2DZ), the basis set also used for the rest of atoms of the compounds involved in this work. Therefore, all of the simulations were conducted at the B3LYP/Lanl2DZ computational level, which has been proved to be reliable for systems involving Pd atoms.[38,39,41−44,49−51,53] Full geometry optimization was performed for isolated reactants, Pd clusters, and reactants−metal systems. Harmonic frequencies were calculated on all optimized structures to confirm the nature of the ground-state stationary point at minima. The palladium atoms present a closed-shell electronic configuration ($4d^{10}$); part of its 4d electronic density must necessarily be promoted into the bordering orbitals, in this case 5s, to enable the formation of a stable metal−metal (Pd−Pd) bond. Therefore, all structures of palladium clusters have been optimized for various accessible spin multiple (singlet and triplet) states.

The stability of palladium clusters was discussed in terms of binding energy (BE), which is defined by equation

$$\mathrm{BE} = \frac{\Delta E}{n} = \frac{-(E_{\mathrm{Pd}_n} - nE_{\mathrm{Pd}})}{n} \quad (1)$$

where ΔE is the stabilization energy by formation of the cluster, obtained from the electronic energies of optimized Pd_n cluster, E_{Pd_n}, and individual Pd atom, E_{Pd}, and n is the number of Pd atoms in the cluster.

The adsorption energy (E_{ads}) per adsorbed intermediate has been defined in terms of the stabilization energy for adsorbate/substrate interaction, calculated according to the expression

$$E_{\mathrm{ads}} = E_{(\mathrm{Pd}_n\ -\ \mathrm{adsorbate})} - (E_{\mathrm{Pd}_n} + E_{\mathrm{adsorbate}}) \quad (2)$$

where E_{Pd_n} and $E_{\mathrm{adsorbate}}$ are the electronic energy of isolated Pd cluster and adsorbate (DCM or H_2), respectively, and $E_{\mathrm{Pd}_n\text{-adsorbate}}$ is the total energy of the optimized Pd_n−DCM system. Hence, a positive E_{ads} value indicates an endothermic adsorption process, whereas a negative one corresponds to an exothermic one. The more negative the adsorption energy, the stronger the adsorption phenomena.

3. RESULTS

3.1. Simulation of Pd Active Species. The first step in the theoretical analysis of DCM HDC was to simulate the active species of the catalyst. For this purpose, we used isolated palladium clusters in quantum-chemical calculations at the B3LYP/Lanl2DZ computational level. Experimental studies have evidenced that the interaction of hydrogen molecules with Pd active sites are strongly dependent on the size of the zerovalent cluster.[73−75] The strategy adopted in this work was to increase the number of palladium atoms of the cluster from 1 to 6 because previous computational studies reported that the BE of Pd_n clusters tend to a constant value for $n > 5$.[33,40,51] In current analysis, we examined the effect of spin multiplicity (singlet and triplet states) and also that of the oxidation state (zerovalent or neutral Pd^0 and electrodeficient Pd^{2+} species) on the molecular properties of Pd_n clusters shown in Scheme 1. The parameters calculated for the simulated Pd active species are collected in Table 1, including total electronic energies, averaged Pd−Pd bond distances, and frequencies of Pd−Pd vibrational tensions and dipolar moments. As can be seen in Figure 1, the relative stability of the Pd^0 clusters, investigated in terms of the BE parameter, increased with the size of the clusters. The results are in agreement with those reported in the literature, which also showed that binding energies of Pd_n clusters remained nearly constant from $n \geq 6$.[33,40] Therefore, for the following analysis of the HDC process, Pd_6 cluster will be used as a model of reference to simulate the Pd active sites of the catalyst. Recent experimental studies showed that Pd clusters grow three-dimensionally over carbon and that when the coverage is increased the particle size is surprisingly diminished because of the polyhedral growth of the clusters.[76,77] Therefore, experimental evidence supports that the octahedral cluster Pd_6 chosen seems to be quite a realistic model for low coverage and highly dispersed Pd clusters over AC. We observed that all triplets structures were significantly more stable than the corresponding ones of singlet state: thus, for Pd_6^0 structures, the triplet state was 7.0 kcal/mol lower in energy than that in singlet state, in agreement with the calculations reported by Kalita,[33] Moc,[38] and Barone.[41] Some minor differences in the symmetry of optimized Pd cluster depending of spin multiplicity were also observed. For example, Pd_6^0 cluster presented, in the singlet configuration, identical lengths for all Pd−Pd bonds, that is, O_h symmetry, whereas in the triplet state, Pd_6^0 cluster is an elongated octahedral structure with D_{4h} symmetry, where two different Pd−Pd bond distances are obtained. In any case, the dipole moments (in debyes) for all stable structures of Pd_n clusters are negligible, indicating spherical charge distribution for the simulated catalytic particles of Pd (Table 1).

To examine the possible role of the oxidation state of Pd on its catalytic activity, we also performed the theoretical study on electrodeficient Pd_n^{2+} clusters, varying n from 1 to 6. (See Table 1.) Similar conclusions as those for neutral Pd cluster were obtained, presenting Pd_n^{2+} clusters with similar bond distances and vibrational frequencies as neutral Pd_n^0 clusters. In addition, Pd_n^{2+} structures with triplet configuration were always

Scheme 1. Molecular Models for Pd_n (n = 2, 3, 4, and 6) Clusters

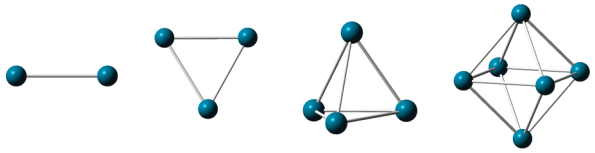

Table 1. Calculated Parameters for Pd_n Clusters Used to Simulate Catalytic Active Species At B3LYP/Lanl2DZ Computational Level

oxidation state	spin multiplicity	cluster (n)	energy (u.a.)	bond[a] length (Å)	freq (cm^{-1})	symmetry	μ (debye)
metallic (Pd^0)	triplet	2	−253.4488	2.53	204.5		0.0
		3	−380.2143	2.65	199.3	C_{2v}	0.4
		4	−507.0106	2.65	232.2	C_s	0.0
		6	−760.5516	2.69	209.0	D_{4h}	0.0
	singlet	2	−253.4362	2.76	130.6		0.0
		3	−380.2048	2.52	250.3	D_{3h}	0.0
		4	−506.9843	2.71	234.4	D_{2d}	0.0
		6	−760.5405	2.70	210.0	O_h	0.0
electrodeficient (Pd^{2+})	triplet	2	−252.6074	2.83	64.8		0.0
		3	−379.3974	2.70	146.9	C_{2v}	0.5
		4	−506.2558	2.72	200.9	C_s	0.0
		6	−759.8629	2.70	210.3	C_{4h}	0.0
	singlet	2	−252.5850	2.62	149.6		0.0
		3	−379.4189	2.72	160.7	D_{3h}	0.0
		4	−506.2074	2.56	248.3	C_s	0.2
		6	−759.8416	2.74	225.6	C_i	0.0

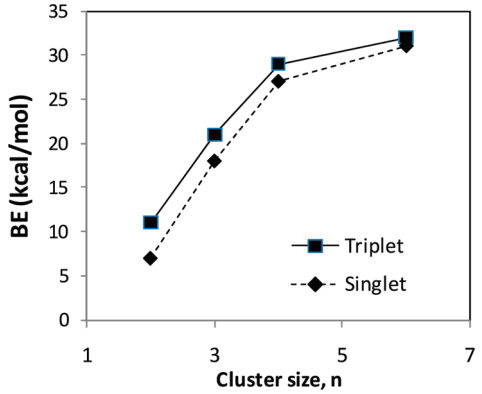

Figure 1. Cluster size effect (n = 2−6) on binding energy (BE) (kilocalories per mole) for Pd_n^0 clusters in singlet and triplet states at B3LYP/Lanl2DZ computational level.

lower in energy (more stable) than those of the singlet state. However, it should be indicated that the optimized geometries of electrodeficient palladium (Pd^{2+}) structures were significantly distorted in symmetry with respect to those of zerovalent Pd_n^0 structures [Pd_6^0(Triplet): C_{4h}; Pd_6^{2+}(Singlet): C_i]

3.2. Interaction of H_2 Molecule with Pd Clusters. Having determined the stable structures for palladium clusters, their interactions with a hydrogen molecule have been considered in this computational analysis because the HDC process involves hydrogen dissociation. The study of Pd_n−H_2 complexes is quite interesting because hydrogenation is one of the main applications of palladium-based catalysts. In general, hydrogen molecules have been demonstrated to be capable of coordinating with Pd_n (n = 2−6) clusters via several ways.[36−42] In this study, we used a computational approach, which introduces the interaction of one H_2 molecule with a Pd_6 cluster as a reference model for Pd active species. The starting point for describing adsorbate−adsorbent interaction in geometry optimization was conducted in four different ways: bond_top, bond_face, bond_bond, and bond_plane, as shown in Scheme 2.

Scheme 2. Different Forms of Interaction for H_2 Molecule with Pd_6 Cluster

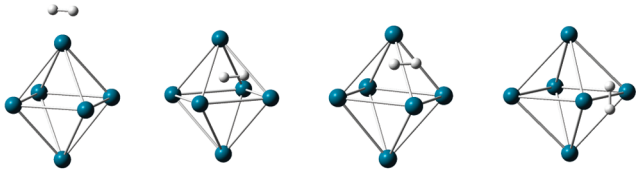

Afterward, we analyzed the ability of palladium clusters to interact and dissociate hydrogen molecule depending of H_2 location at Pd cluster surface. Figure 2 shows the equilibrium geometries for Pd_6^0−H_2 complexes and the corresponding adsorption energy (E_{ads}) as a function of the approach between the adsorbate (hydrogen molecule, H_2) and adsorbent (Pd_6^0 clusters in singlet and triplet state) used in quantum chemical calculations. As can be seen, for both Pd_6^0(Triplet)−H_2 and Pd_6^0(Singlet)−H_2 systems, the interaction of hydrogen molecule through the bond_top of the Pd cluster did not promote dissociation, even when the H−H distance in Pd_n−H_2 system was elongated around 0.06 Å in relation to that of isolated H_2 molecule. Calculations evidenced similar evolution for triplet and singlet states of Pd_n−H_2 structures from bond_top approach, yielding adsorption energy (E_{ads}) values of −8.1 and −6.1 kcal/mol for Pd_6^0(Triplet)−H_2 and Pd_6^0(Singlet)−H_2 systems, respectively, and differing only in some geometric details. These results indicate the possibility of physical adsorption of the hydrogen molecule on the surface of active Pd species in both triplet (more energetically favored) and singlet states.

In contrast, the other routes of approaching (bond_face, bond_bond, and bond_plane) between H_2 molecule and Pd_6^0 cluster imply a complete dissociation of the hydrogen molecule for both singlet and triplet states, as shown in Figure 2. In general, the most stable Pd_6^0−H_2 complexes presented the dissociated hydrogen atoms chemically adsorbed on the palladium triangle

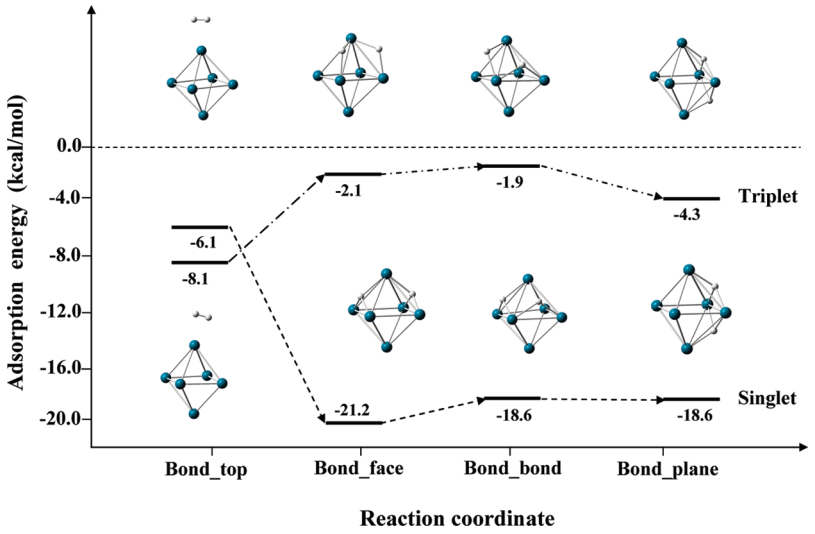

Figure 2. Adsorption energies (kilocalories per mole) and geometries for optimized ($Pd_6^0-H_2$) species resulting from the adsorption of hydrogen molecule on metallic palladium Pd_6^0(Singlet) and Pd_6^0(Triplet) clusters as a function of the adsorbate−adsorbent approach followed in the B3LYP/Lanl2DZ calculations.

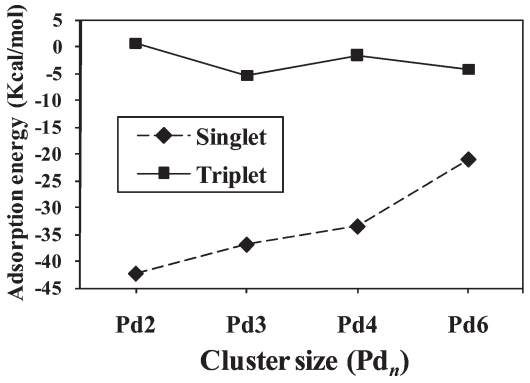

Figure 3. Cluster size effect (n = 2−6) on adsorption energy (kilocalories per mole) for $Pd_n^0-(H_2$ dissociated) complexes in singlet and triplet states at the B3LYP/Lanl2DZ computational level.

planes. However, significant differences in adsorption energy between Pd_6^0(Singlet)−(H_2dissociated) and Pd_6^0(Triplet)−(H_2dissociated) species can be noticed. (See Figure 2.) Therefore, the singlet spin configuration of Pd_6^0 cluster strongly favored the H_2 dissociation by Pd active site, yielding high adsorption energy. Meanwhile, H_2 in the Pd_6^0(Triplet) cluster dissociates without significant energetic stabilization. As shown in a previous section, the isolated Pd_6^0 was 7.0 kcal/mol more stable in the triplet than in the singlet state. Then, the energetically accessible Pd active species in the catalyst would preferably be in the triplet state. Therefore, the dissociation of H_2 by Pd should evolve through a spin multiplicity change in the reaction pathway, which was also revealed by CASPT calculations.[41] In any case, current results indicated that the dissociated hydrogen species should be very close in energy to the system with physically adsorbed H_2 molecules.

To analyze the possible influence of Pd cluster size on H_2 dissociation, we show in Figure 3 the size dependence of hydrogen dissociative adsorption using the most stable $Pd_n^0-(H_2$ dissociated) structures in our study, which were found through the approach named bond_face using the E_{ads} parameter defined by eq 2. We observed that an increase in the number of palladium atoms does not significantly affect the stability of Pd_n^0-(Triplet)−H_2 complexes. Pd_n^0(Singlet) clusters yielded lower adsorption energies of DCM when the number of constituent Pd atoms increases until n = 6, reducing the energetic differences between singlet and triplet states. This effect of the Pd particle size was experimentally observed by Huang et al.,[73] who demonstrated that the heat value of exothermic chemisorption of H_2 on Pd samples raised abruptly when decreasing the particle diameter of metal to subnanometer. In fact, experimental values of H_2 chemisorption heat for Pd particle size <1 nm were in the range of 20−45 kcal/mol,[73] in fairly good agreement with the results of calculations in Figure 3.

Once confirmed, the suitability of our computational method for describing the dissociation of H_2 by zerovalent Pd particles, we introduced in the analysis the interaction between one H_2 molecule and electrodeficient Pd_6^{2+} clusters because the presence of Pd^{2+} has been experimentally related to the catalyst activity in HDC of DCM.[2−6] To the best of our knowledge, the effect of oxidation state of Pd on the catalytic activity in hydrogenation reactions has never been theoretically studied before. Figure 4 shows the equilibrium geometries of the complex ($Pd_6^{2+}-H_2$) together with the adsorption energies as a function of the starting approach between hydrogen molecule and Pd_6^{2+} cluster for both singlet and triplet states in the optimization calculations carried out by quantum chemical calculations. (See Scheme 2.) The results indicate that Pd^{2+} also dissociates the hydrogen molecule, yielding even stronger stabilization of the reactive intermediate on the catalyst surface. In good concordance with theoretical results for neutral Pd cluster, the only exceptions were the adsorbed hydrogen molecule H_2 through the bond_top position at Pd_6^{2+}(Singlet) and Pd_6^{2+}(Triplet) clusters, which did not involve the dissociation of hydrogen molecule. The results for Pd_6^{2+}-(Triplet)−H_2 system through bond_top approach (Figure 4) cannot be rigorously considered as physical adsorption because the adsorption energy is fairly high (−25 kcal/mol), closer to the values for chemical adsorption of the dissociated complexes.

The rest of the routes for H_2 approaching Pd_6^{2+}(Singlet) and Pd_6^{2+}(Triplet) structures imply the complete dissociation of the

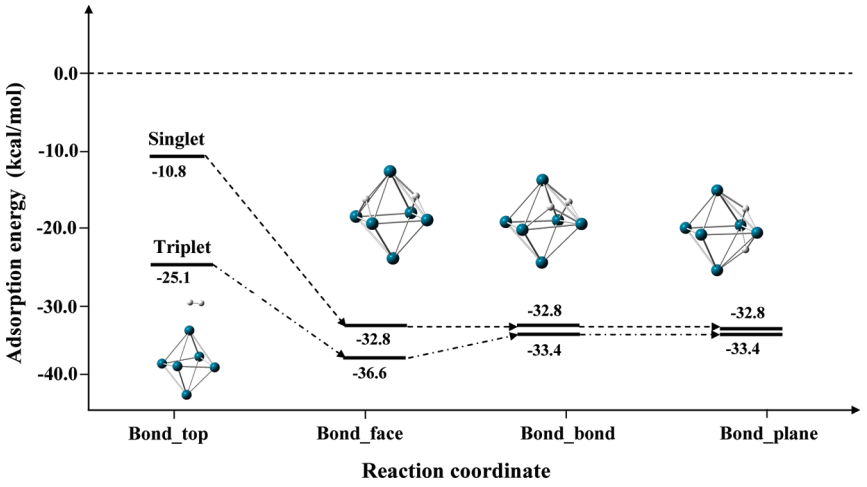

Figure 4. Adsorption energies (kilocalories per mole) and geometries for optimized ($Pd_6^{2+}-H_2$) species resulting from the adsorption of hydrogen molecule on electrodeficient Pd_6^{2+}(Singlet) and Pd_6^{2+}(Triplet) palladium clusters as a function of the adsorbate−adsorbent approach followed in the B3LYP/Lanl2DZ calculations.

Scheme 3. Different Forms of Interaction for DCM with the Pd_6 Cluster

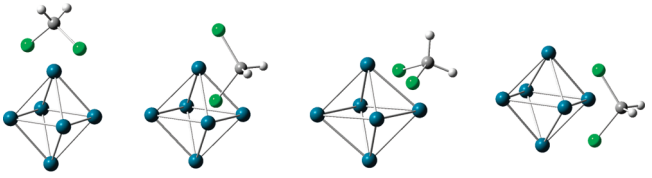

hydrogen molecule, having $Pd_6^{2+}-(H_2$ dissociated) complexes with very similar stabilization energies in both spin configurations. Compared with the zerovalent Pd_6^0 case, the dissociation of hydrogen compounds by electrodeficient Pd_6^{2+} was found to be more energetically favored (compare results in Figures 2 and 4). Therefore, theoretical results indicate that the electrodeficient Pd^{2+} species interacts more effectively with the hydrogen molecule, resulting in a more energetically stabilized dissociated H intermediates.

3.3. Interaction of DCM Molecule with Pd Clusters. The interaction between Pd_6 and DCM has been promoted by approaching DCM at different active sites of the Pd cluster surface (bond_top, bond_face, bond_bond, and bond_plane), as in Scheme 3. The possible adsorption/reaction was first examined on zerovalent Pd_6^0 cluster for both triplet and singlet electronic spin configurations. Figure 5 presents the local minima configurations for the different DCM molecule approaching modes toward Pd_6^0, together with the adsorption energies for the resulting Pd_6^0-DCM systems. In contrast with the previous study of H_2 adsorption on Pd clusters, the most stable adsorbed Pd_6^0-DCM structures always correspond to triplet state. These results discard the possibility of spin multiplicity change during adsorption phenomena; as consequence, subsequent theoretical analysis will be centered on Pd_6^0(Triplet) active species. As can be observed in Figure 5, fairly different Pd_6^0(triplet)−DCM structures are obtained depending on the way DCM approaches the Pd_6^0 cluster. Therefore, when DCM approaches the top (bond-top) or the triangular face center (bond-face) of octahedron Pd structure, it is physically adsorbed around the Pd atoms, with very similar stabilization energies (near −6 kcal/mol), and dissociation of chlorine atoms is not achieved. However, if DCM approaches the bridge site of Pd_6^0 cluster, then it could partially dissociate with one chlorine atom adsorbed on the triangular face of Pd_6^0 structure, which is only slightly distorted by the reactive adsorption of DCM. However, the most stable Pd_6^0-DCM complexes in this study are obtained when the geometry optimization starts from bond-plane approach. In this case, the fragmentation of DCM involves the concerted shift of both chlorine atoms toward the center of nonadjacent triangular faces of Pd_6^0 cluster. Scheme 4 illustrates more clearly the optimized Pd_6^0-DCM complex for the complete dissociative adsorption of DCM on Pd cluster. It is remarkable that the complete breakdown of one or two C−Cl bonds in DCM (from 1.85 Å in the isolated compound to 3.38 Å in the dissociated adsorbed species in Table 2) ocurrs progressively through the formation of one or two new Pd−C bonds between the methylene group and the Pd atoms on cluster surface, with bond distances as short as 1.96 Å. (See Table 2.) This finding is consistent with the significantly higher stabilization energies (−46 and −54 kcal/mol) for the dissociative chemisorption of DCM on Pd_6^0 with respect to those obtained for H_2. (See Figure 2.) As can be appreciated in Figure 5, the octahedron structure of Pd_6^0 cluster is scarcely modified by the DCM dissociation on its surface, the mean Pd−Pd bond distance remaining around 2.7 to 2.8 Å.

Therefore, according to the computational results presented here, both physical and chemical adsorption of DCM (the latter with partial and total dissociation) may occur on the palladium surface at low temperature. The dissociative adsorption of DCM on Pd at low temperatures (243 K) has been previously evidenced by means of infrared spectroscopy combined with mass spectrometry by comparing the spectra of DCM in the gas phase and on the surface of Pd.[78] In current work, theoretical predictions for absorption bands of DCM_{gas} and Pd_6-DCM complex are used to analyze the empirical assignments performed by Solymosi and Rasko.[78] As a result, Table 3 compares experimental and theoretical vibrational frequencies for gaseous DCM, showing that the computational approach reasonably describes the bands observed by IR spectroscopy. As can also

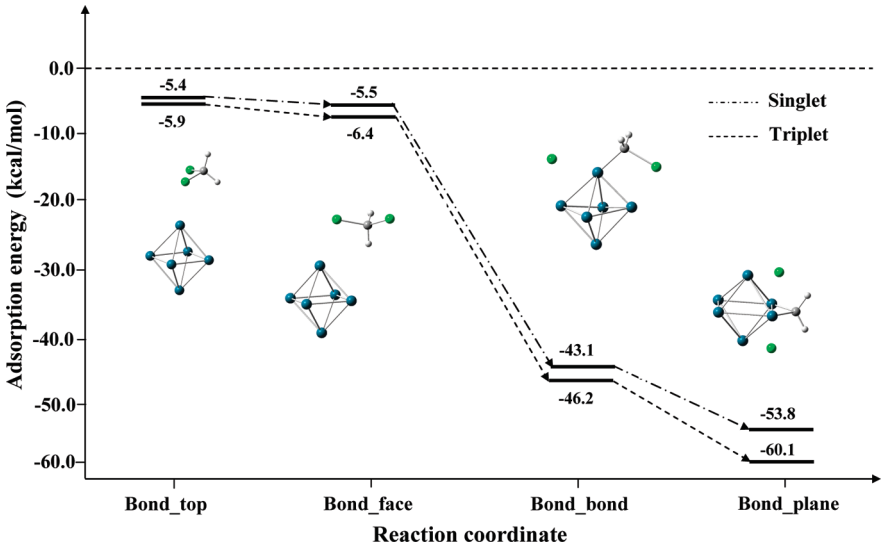

Figure 5. Adsorption energies (kilocalories per mole) and geometries for optimized (Pd_6^0—DCM) species resulting from the adsorption of dichloromethane molecule on neutral palladium Pd_6^0(Singlet) and Pd_6^0(Triplet) clusters as a function of the adsorbate—adsorbent approach followed in the B3LYP/Lanl2DZ calculations.

Scheme 4. Different Views of Optimized Geometry of Adsorbed DCM-Pd_6 Intermediate Obtained from the Complete Dissociative Adsorption

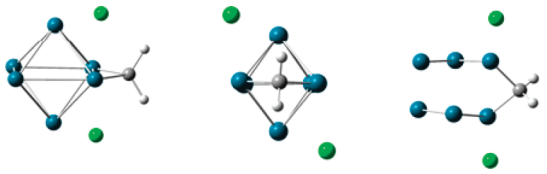

be seen in Table 3, the spectrum of DCM on Pd surface shows spectral features significantly different from those of the DCM gas spectrum. The frequencies of both symmetric and asymmetric CH_2 tension modes [$\nu_{s/as}(CH_2)$] and, more significantly, CH_2 deformation mode [$\delta(CH_2)$] are shifted to low frequencies by interaction with Pd surface. Solymosi and Rasko[78] tentatively ascribed the new bands at 2984 and 2907 cm^{-1}, respectively, to the asymmetric and symmetric stretches of CH_2 species formed in the dissociative adsorption of DCM on Pd. As can be seen in Table 3, those empirical assignments are fully confirmed by density functional calculations of chemisorbed DCM on Pd_6^0 cluster, which identifies CH_2 as the primary product of DCM dissociation. The formation of the Pd_6^0—DCM complex also implies the disappearance of $\nu_{as}(C-Cl_2)$ and $\nu_s(C-Cl_2)$ bands, which are neither observed in experimental spectrum. This is an additional spectroscopic proof of the complete breakdown of C—Cl bond in DCM by dissociative adsorption on Pd, which is represented in Figure 5. In fact, according to the computational results, very intense infrared signals related to the new Pd—C and Pd—Cl vibrational modes should be observed in the 600—200 cm^{-1} spectral zone, which is out of the range measured by Solymosi and Rasko.[78] Experimental and theoretical evidence of the dissociative adsorption of the analogous CH_2I_2 compound on metal surfaces of Pd,[79] Rh,[80] and Ag[81] have also been reported, again identifying methylene intermediates involved in the catalytic destruction of halogenated hydrocarbon. It is generally accepted in the literature that the adsorption of chlorofluorcarbons on palladium surface is dissociative.[82] Fung et al.[83] demonstrated the ability of metals as Ag to form metal—chlorine bonds through the chemisorption of chlorinated molecules as methyl chloride (CH_3Cl), with the associated breakdown of C—Cl bonds. Additional experimental evidence of the strong interaction between CH_2 group and two adjacent Pd atoms (as those shown in Figure 5 and Scheme 4) is the route of the synthesis of Pd_2(μ-bis(diortho-tolyphosphino)methane)$_2$, shown in Scheme 5.[84] Thus, complex 1 readily adds DCM to form the new methylene-bridged complex 2, where the two chlorine atoms are dissociated from DCM and located over Pd atoms, whereas the methylene group is chemically linked to the two near Pd atoms of Pd_2 P_4 unit.

DFT analysis of the interaction of Pd^0 with DCM has revealed that DCM can be physically or chemically adsorbed by neutral palladium, depending on the surface position of that interaction. Now, we will extend the theoretical study to the interaction between DCM and electrodeficient palladium (Pd^{2+}) clusters to obtain a deeper insight into the role of electrodeficient Pd^{2+} active species in the activity, selectivityn and stability of the catalyst in HDC reaction. For this purpose, the adsorption of DCM at four possible sites (bond_top, bond_face, bond_bond, and bond_plane) of electrodeficient Pd_6^{2+}(Triplet) cluster has been systematically investigated. On the basis of the adsorption energies of DCM and the equilibrium geometries of the optimized Pd_6^{2+}(Triplet)—DCM intermediates, a thermodynamic scheme of DCM adsorption on electrodeficient palladium (Pd^{2+}) was developed, as shown in Figure 6. As for the case of zerovalent Pd_6^0 cluster, we have found two forms of nondissociative adsorption of DCM (corresponding to bond_top and bond_face approaches) as well as partial and complete dissociation of DCM (corresponding to bond_bond and bond_plane approaches, respectively) over Pd_6^{2+}(Triplet) surface. The high adsorption energy (about −50 kcal/mol, see Figure 6) for the nondissociated Pd_6^{2+}(Triplet)—DCM structures, approaching by bond_face, corresponds to a chemical adsorption rather than physical interaction. The partial and complete dissociation of chlorine atoms of DCM on Pd_6^{2+} surface evolves without

Table 2. Bond Length (angstroms) for Optimized Structures of Isolated and Adsorbed DCM in Pd_6 in Triplet State at B3LYP/Lanl2DZ Computational Level

	independent species				nondissociative adsorption				complete dissociation			
bond (Å)	Pd−C	Pd−Cl	C−Cl	Pd−Pd	Pd−C	Pd−Cl	C−Cl	Pd−Pd	Pd-C	Pd−Cl	C−Cl	Pd−Pd
Pd_6^0(T)			1.85	2.69	3.76	2.71	1.88	2.72	1.96	2.60	3.38	2.81
Pd_6^{2+}(T)			1.85	2.70	3.82	2.69	1.88	2.81	1.98	2.50	3.45	3.16

Table 3. Vibrational Frequencies (in inverse centimeters) of DCM in the Gas Phase and on the Pd Surface (Obtained by Dissociative Adsorption) Obtained Experimentally (Ref 50) and Calculated at B3LYP/Lanl2DZ Computational Level

	DCM_{gas}		$DCM_{adsorbed\ on\ Pd}$	
vibrational mode	DCM^{exptl}	DCM^{theor}	DCM/Pd^{exptl}	DCM/Pd^{theor}
$\nu_{as}(CH_2)$	3045	3282	2984	3175
$\nu_s(CH_2)$	3007	3173	2907	3042
$\delta(CH_2)$	1473	1454	1426	1342
CH_2wag	1275	1300	?	972
$\rho(CH_2)$	898	891	?	738
$\nu_{as}(C-Cl_2)$	758	679		
$\nu_s(C-Cl_2)$	707	650		
ν_s(Pd−C)			?	579
ν_{as}(Pd−C)			?	576
ν_{as}(Pd−Cl)			?	253
ν_s(Pd−Cl)			?	251

Scheme 5. Synthesis of Pd_2 (μ-Bis(di-*ortho*-tolyphosphino)-methane)$_2$ in Ref 56

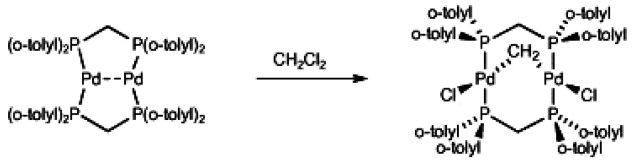

Complex **1** Complex **2**

significant barrier of energy and presents high stabilization (about −50 kcal/mol), similar to that found for the dissociative adsorptions of DCM on zerovalent Pd_6^0 cluster. Regarding the effect of dissociative DCM adsorption on Pd_6^{2+} particle, it is remarkable that the significant distortion of the octahedron structure of Pd cluster due to local relaxation of the surface to form the dissociated Pd_6^{2+}(Triplet)−DCM complex, as reflected by the mean Pd−Pd distance in Table 2. In contrast, other structural parameters (C−Cl and Cl−Pd) associated with DCM adsorbed species are very similar for Pd_6^0 and Pd_6^{2+} cases (Table 2).

In the previous section, we analyzed the dependence of the Pd_n cluster size on the adsorption energies of H_2 on palladium surface. In Figure 7, the comparison of the cluster size effect on dissociative adsorption of DCM is presented for both zerovalent Pd_n^0 and electrodeficient Pd_n^{2+} structures in the triplet state. As can be seen, Pd_6^0 and Pd_6^{2+} clusters present similar ability to generate dissociated DCM-Pd intermediates, which are highly favored thermodynamically independently of the cluster size.

3.4. Analysis of DCM Hydrodechlorination with Pd-Based Catalyst from DFT Calculations. In this work, density functional calculations have been performed to investigate the interaction of both reactants (H_2 and DCM) involved in HDC reaction using Pd-based catalysts. The molecular model used to simulate Pd active species consists of subnanometer Pd_6 cluster, representing a catalyst with extremely dispersed particles (then neglecting the influence of the support on the activity). Despite this simplification, some relevant information has been achieved regarding the elementary processes that occur when gaseous H_2 and DCM molecules interact with surface Pd atoms. To overview current theoretical results, we present in Figure 8 the adsorption enthalpy values for the reaction pathway describing the activation of H_2 and DCM over Pd_6 surfaces, given as adsorption enthalpy values, considering the possible presence of both zerovalent and electrodeficient Pd species in the catalyst. Table 4 completes the thermodynamic description of H_2 and DCM adsorption on Pd cluster collecting electronic stabilization energies, enthalpies, and free energies for those phenomena, as obtained by DFT calculations.

As we noted, depending on the site of interaction with Pd_6 cluster, H_2 is physically adsorbed around Pd atoms, or, in other cases, H_2 is dissociated. According to the DFT results, the triplet species is 7 kcal/mol more stable than the singlet species. Therefore, activated H_2 dissociation on Pd_6^0 structure includes the triplet−singlet transition induced by the spin−orbit interaction as a key step. The theoretical H_2 dissociation enthalpy obtained for cluster reasonably agrees with the experimental values (20−25 kcal/mol).[85] Consistently with this low adsorption enthalpy, it has been experimentally demonstrated that Pd clusters reversibly adsorb and desorb hydrogen.[73] The weak Pd−H bond would allow the chemisorbed H atoms to react with other adsorbed species. The dissociation of H_2 on electrodeficient Pd_6^{2+} cluster involves only the triplet state. Attending to the reaction enthalpies, the electrodeficient palladium species present a higher capacity to dissociate the H_2 molecule, involving more stabilized H-intermediates. As a consequence, the H_2 adsorbed on Pd_6^{2+} structures should be more energetically demanding for desorption or subsequent reaction steps.

Recently, de Pedro et al.[4] reported a kinetic study on HDC of DCM with Pd/AC catalyst[4] based on fixed bed reactor experiments. The results allowed us to conclude that DCM adsorption onto the active sites is the rate-controlling step. From the evolution of DCM and the reaction products, the reaction pathway shown in Scheme 6 was proposed, which implies the formation of adsorbed intermediates (CH_2Cl^*, $CH_2{}^{**}$, and $C_2H_4{}^{**}$ species), yielding CH_4, CH_3Cl, and C_2H_6 as reaction products. As shown in Figures 8 and 5, theoretical calculations confirm the presence of the thermodynamically favored

dx.doi.org/10.1021/jp200329j |J. Phys. Chem. C 2011, 115, 14180–14192

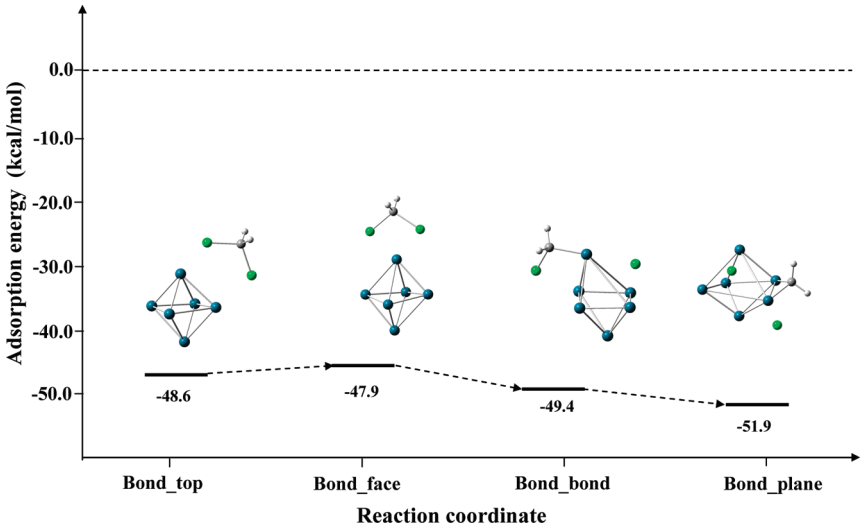

Figure 6. Adsorption energies (kilocalories per mole) and geometries for optimized (Pd_6^{2+}—DCM) species resulting from the adsorption of dichloromethane molecule on electrodeficient Pd_6^{2+}(Triplet) clusters as a function of the adsorbate—adsorbent approach followed in the B3LYP/Lanl2DZ calculations.

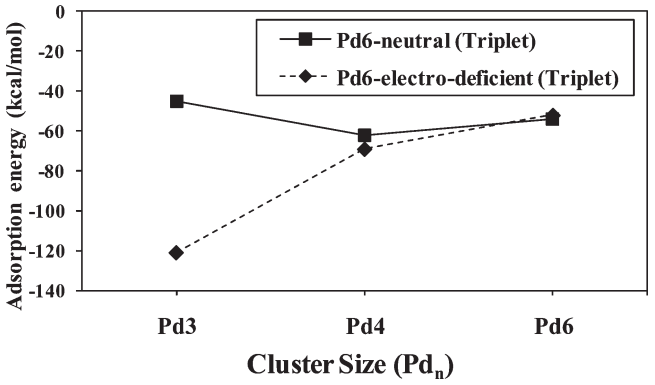

Figure 7. Cluster size effect (n = 2—6) on adsorption energy (kilocalories per mole) for dissociative adsorption of DCM on Pd_n^0 and Pd_n^{2+} clusters in triplet state at B3LYP/Lanl2DZ computational level.

CH_2Cl^* and CH_2^{**} species adsorbed on Pd surface. In fact, partially and fully dissociated DCM—Pd complexes may be formed through independent pathways according to DFT optimizations for both zerovalent and electrodeficient Pd clusters in the triplet state, with high adsorption enthalpies (<−50 kcal/mol) and without activation barriers. Therefore, current theoretical results indicate that the dissociative adsorption of DCM on Pd active sites occurs via the scission of one or two C—Cl bonds, promoted by the formation of one or two C—Pd linkages, respectively. This suggests the possibility of considering a new independent single step (marked by dot line) in Scheme 6 for the direct formation of carbene (CH_2^{**}) intermediate, providing a parallel scheme for CH_3Cl and CH_4 (or C_2 hydrocarbons) formation. This is in agreement with the findings of previous experimental studies,[3,4] where a parallel scheme was proposed for the HDC of chloromethanes. Moreover, the fact that the CH_2^{**} species appear to be the most energetically favored intermediate in DCM adsorption on Pd surface (as explained above) seems to be consistent with the high selectivity to CH_4 found in HDC reactions with Pd/AC catalysts.[2—5]

The dissociative adsorption of chlorinated compounds over Pd surface as the HDC rate-determining step is consistent with the general trend observed for the reactivity of chloromethanes (CCl_4 > $CHCl_3$ > CH_2Cl_3> CH_3Cl).[3] To analyze this point, we here extend DFT calculations to the interaction of $CHCl_3$ and CH_3Cl with Pd_6^0 and Pd_6^{2+} clusters in the triplet state. As can be seen in Table 5, the exothermic character of the dissociative adsorption of chloromethanes decreases as the number of chlorine atoms in the molecule diminishes, in the same order as HDC reactivity, thus supporting experimental observations. Experiments carried out with different Pd/AC catalysts (prepared using different palladium precursors) showed lower DCM conversions as the relative amount of electrodeficient palladium (Pd^{n+}) in the catalyst decreases. This may be related with the higher stabilization energies of the dissociated DCM intermediates on zerovalent Pd_6^0 clusters with respect to those on electrodeficient Pd_6^{2+} (Table 4), giving rise to lower reaction rates.

Previous experimental work[5] demonstrated that the active centers of Pd/AC catalysts are constituted by the association of electrodeficient (Pd^{n+}) and zerovalent (Pd^0) palladium. Pd/AC catalysts yield very good results in terms of activity and selectivity to nonchlorinated compounds, but they undergo severe deactivation after a few hours of operation. Experimental evidence[2,3] ascribed the significant deactivation to the poisoning of Pd active centers with organochlorinated compounds. However, relationships between the structure and the activity of Pd/AC catalysts have not been largely analyzed. There was found, however, that catalyst deactivation was clearly related to the great decrease in the accessible electrodeficient Pd species upon use in HDC. Theoretical results in this work show that DCM can be molecularly adsorbed on both zerovalent and electrodeficient Pd. However, we found that the nondissociative adsorption of DCM over electrodeficient Pd_6^{2+} cluster is remarkably favored in energy (Table 4), with adsorption enthalpies (∼ −50 kcal/mol) corresponding to chemical adsorption and one order of magnitude larger than the values for physical adsorption of DCM on zerovalent Pd_6^0 cluster. Current results explain the deactivation of Pd/AC catalyst as a consequence of the selective poisoning

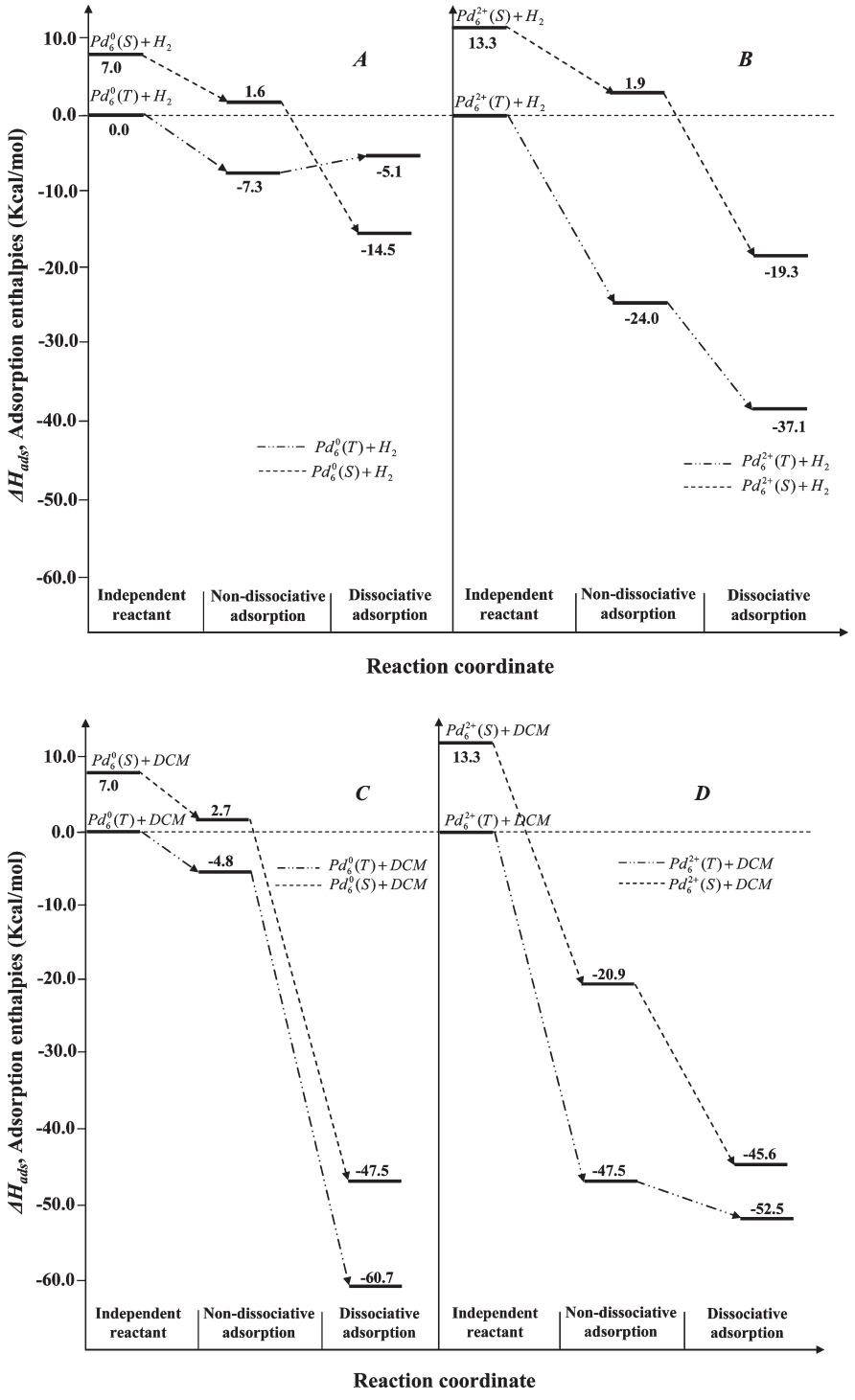

Figure 8. Profiles of ΔH_{ads} (298.15 K) for activation of H_2 by (A) Pd_6^0 and (B) Pd_6^{2+} clusters and for activation of DCM by (C) Pd_6^0 and (D) Pd_6^{2+} clusters.

of electrodeficient Pd active centers by chlorinated hydrocarbons, in complete agreement with the experimental findings. In fact, Table 5 shows that the nondissociative chemical adsorption of chloromethanes on electrodeficient Pd_6^{2+} active sites is thermodynamically favored in the order DCM > MCM > TCM, which confirms the unexpected order of Pd/AC catalyst deactivation experimentally found for the HDC of those compounds.[3]

However, the thermodynamic data of Tables 4 and 5 cannot be conclusively used to explain the experimental evidence relative to Pd/AC activity and, especially, selectivity to the different HDC products (CH_4, CH_3Cl, C_2H_6, and C_3H_8) from DCM. Further computational studies involving transition states must be carried out in future works to evaluate energy barrier for going from adsorbed H_2 and DCM intermediates to HDC products, and these calculations should be extended to molecular models of

Table 4. Calculated Thermodynamic Parameters (kilocalories per mole) for DCM Adsorption on Pd Clusters Calculated at B3LYP/Lanl2DZ Computational Level

kcal/mol		reactants			physical adsorption			dissociative adsorption		
		E_{ads}	ΔH_{ads}	ΔG_{ads}	E_{ads}	ΔH_{ads}	ΔG_{ads}	E_{ads}	ΔH_{ads}	ΔG_{ads}
H_2	Pd_6^0(Singlet)	7.0	7.0	10.1	−0.8	1.6	9.2	−14.2	−14.5	−5.3
	Pd_6^0(Triplet)	0	0	0	−8.1	−7.3	−1.6	−4.3	−5.1	2.6
	Pd_6^{2+}(Singlet)	13.4	13.3	11.8	0.6	1.9	7.9	−19.4	−19.3	−12.6
	Pd_6^{2+}(Triplet)	0	0	0	−25.1	−24.0	−18.6	−36.6	−37.1	−30.4
DCM	Pd_6^0(Singlet)	7.0	7.0	10.1	1.6	2.7	11.1	−46.8	−47.5	−34.8
	Pd_6^0(Triplet)	0	0	0	−5.9	−4.8	1.2	−60.1	−60.7	−48.6
	Pd_6^{2+} (Singlet)	13.4	13.3	11.8	−21.9	−20.9	−12.4	−44.7	−45.6	−37.3
	Pd_6^{2+}(Triplet)	0	0	0	−48.6	−47.5	−38.6	−51.9	−52.5	−43.2

Scheme 6. Reaction Scheme for HDC of DCM Proposed in Ref 4[a]

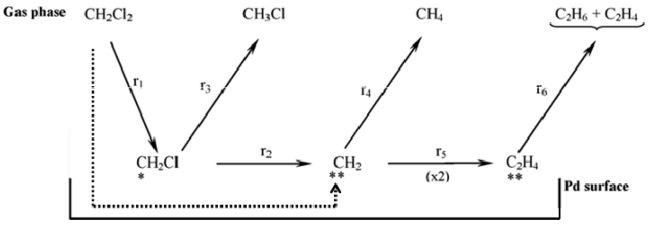

[a] Dotted line indicates the proposed new reaction pathway from current DFT calculations.

Table 5. Calculated Thermodynamic Parameters (kilocalories per mole) for Dissociative Adsorption of Chloromethane Compounds on Pd Clusters Calculated at B3LYP/Lanl2DZ Computational Level

kcal/mol		nondissociative adsorption			dissociative adsorption		
		E_{ads}	ΔH_{ads}	ΔG_{ads}	E_{ads}	ΔH_{ads}	ΔG_{ads}
MCM	Pd_6^0(Triplet)	−6.9	−6.3	2.3	−28.4	−29.3	−18.4
	Pd_6^{2+}(Triplet)	−42.9	−42.4	−33.9	−26.1	−26.4	−19.3
DCM	Pd_6^0(Triplet)	−5.9	−4.8	1.2	−60.1	−60.7	−48.6
	Pd_6^{2+}(Triplet)	−48.6	−47.5	−38.6	−51.9	−52.5	−43.2
TCM	Pd_6^0(Triplet)	−5.4	−5.0	4.7	−63.8	−64.3	−50.6
	Pd_6^{2+}(Triplet)	−41.9	−41.6	−31.6	−67.9	−67.8	−59.7

catalyst including support atoms to achieve deeper insight into the activity and selectivity of Pd/AC catalysts, the roles of the support and Pd^{n+}/Pd^0 ratio.

4. CONCLUSIONS

An attempt for the molecular simulation of DCM HDC with palladium catalyst has been carried out at B3LYP/Lanl2DZ computational level. For this purpose, the DFT analysis focused on the interactions of DCM and H_2 reactants with the surface of Pd catalyst, using molecular models with different cluster size, oxidation state, and spin configuration. Theoretical results show that the HDC mechanism involves the dissociative adsorption of both DCM and H_2 reactants on Pd surface, in good agreement with experimental evidence. Remarkably, calculations show that the partial and complete C−Cl dissociations of DCM by Pd clusters are promoted by the formation of C−Pd linkages, implying much higher adsorption enthalpies than for the case of H_2 activation by Pd species. As relevant computational results, we find that the nondissociative adsorption of DCM over electrodeficient Pd cluster presents remarkably higher adsorption enthalpy than over zerovalent Pd cluster; the former is coherently described as chemical adsorption. This theoretical evidence explains the severe deactivation of Pd/AC catalyst as a consequence of the selective poisoning of electrodeficient Pd active centers by chlorinated hydrocarbons, which is favored in energy in the order DCM > MCM > TCM, consistently with our previous experimental findings.

Future computational studies will focus on transition states for going from adsorbed H_2 and DCM intermediates to HDC products to estimate energy barriers and achieve a deeper insight into the activity and selectivity of Pd-based catalysts and their dependence on the reaction temperature and Pd^{n+}/Pd^0 ratio.

■ ACKNOWLEDGMENT

We are grateful to the Spanish "Ministerio de Ciencia e Innovación" and "Comunidad de Madrid" for financial support (CTQ2008-04751, CTQ2008-05641, and S2009/PPQ-1545). We are also very grateful to "Centro de Computación Científica de la Universidad Autónoma de Madrid" for computational facilities.

■ REFERENCES

(1) Anastas, P. T.; Kirchhoff, M. M. *Acc. Chem. Res.* **2002**, *35*, 686.
(2) Alvarez-Montero, M. A.; Gomez-Sainero, L. M.; Juan-Juan, J.; Linares-Solano, A.; Rodriguez, J. J. *Chem. Eng. J.* **2010**, *162*, 599.
(3) Alvarez-Montero, M. A.; Gomez-Sainero, L. M.; Martin-Martinez, M.; Heras, F.; Rodriguez, J. J. *Appl. Catal., B* **2010**, *96*, 148.
(4) de Pedro, Z. M.; Casas, J. A.; Gomez-Sainero, L. M.; Rodriguez, J. J. *Appl. Catal., B* **2010**, *98*, 79.
(5) de Pedro, Z. M.; Gomez-Sainero, L. M.; Gonzalez-Serrano, E.; Rodriguez, J. J. *Ind. Eng. Chem. Res.* **2006**, *45*, 7760.
(6) Gomez-Sainero, L. M.; Seoane, X. L.; Arcoya, A. *Appl. Catal., B* **2004**, *53*, 101.
(7) *Annual Toxics Release Inventory Data Release Report; Office of Pollution Prevention and Toxics, U. S.*; Environmental Protection Agency: Washington, DC, 1999.

(8) *Handbook of Pesticide Toxicology*; Hayes, W. J., Laws, E. R., Eds.; Academic Press: San Diego, 1991; Vol. 1.
(9) Dobrzynska, E.; Posniak, M.; Szewczynska, M.; Buszewski, B. *Crit. Rev. Anal. Chem.* **2010**, *40*, 41.
(10) Cheremisinoff, N. P. *Industrial Solvents Handbook*, 2nd ed.; Marcel Dekker, Inc.: New York, 2003.
(11) Wiersma, A.; van de Sandt, E. J. A. X.; den Hollander, M. A.; van Bekkum, H.; Makkee, M.; Moulijn, J. A. *J. Catal.* **1998**, *177*, 29–39.
(12) Makkee, M.; Wiersma, A.; van de Sandt, E. J. A. X.; van Bekkum, H.; Moulijn, J. A. *Catal. Today.* **2000**, *55*, 125–137.
(13) Urbano, F. J.; Marinas, J. M. *J. Mol. Catal. A: Chem.* **2001**, *173*, 329–345.
(14) Gomez-Sainero, L. M.; Seoane, X. L.; Fierro, J. L. G.; Arcoya, A. *J. Catal.* **2002**, *209*, 279–288.
(15) Babu, N. S.; Lingaiah, N.; Pasha, N.; Kumar, J. V.; Prasad, P. S. S. *Catal. Today* **2009**, *141*, 120–124.
(16) Ding, E.; Jujjuri, S.; Sturgeon, M.; Shore, S. G.; Keane, M. A. *J. Mol. Catal. A: Chem.* **2008**, *294*, 51–60.
(17) Cobo, M. I.; Conesa, J. A.; de Correa, C. M. *J. Phys. Chem. A* **2008**, *112*, 8715–8722.
(18) Jujjuri, S.; Ding, E.; Hommel, E. L.; Shore, S. G.; Keane, M. A. *J. Catal.* **2006**, *239*, 486–500.
(19) Ordonez, S.; Diaz, E.; Bueres, R. F.; Asedegbega-Nieto, E.; Sastre, H. *J. Catal.* **2010**, *272*, 158–168.
(20) Ordonez, S.; Diez, F. V.; Sastre, H. *Appl. Catal., B* **2001**, *31*, 113–122.
(21) Ribeiro, F. H.; Gerken, C. A.; Rupprechter, G.; Somorjai, G. A.; Kellner, C. S.; Coulston, G. W.; Manzer, L. E.; Abrams, L. *J. Catal.* **1998**, *176*, 352–357.
(22) Gomez-Quero, S.; Cardenas-Lizana, F.; Keane, M. A. *Ind. Eng. Chem. Res.* **2008**, *47*, 6841–6853.
(23) Bae, J. W.; Lee, J. S.; Lee, K. H. *Appl. Catal., A* **2008**, *334*, 156–167.
(24) Álvarez-Montero, M. A.; Gómez-Sainero, L. M.; Mayoral, A.; Diaz, I.; Baker, R. T.; Rodriguez, J. J. *J. Catal.* **2011**, *279*, 389–396.
(25) Thompson, C. D.; Rioux, R. M.; Chen, N.; Ribeiro, F. H. *J. Phys. Chem. B* **2000**, *104*, 3067–3077.
(26) Radovic, L. R.; Moreno-Castilla, C.; Rivera-Utrilla, J. In *Carbon Materials As Adsorbents in Aqueous Solution*; Radovic, L. R., Ed.; Chemistry and Physics of Carbon 27; Marcel Dekker: New York, 2000; pp 227−405.
(27) Gonzalez, C. A.; Bartoszek, M.; Martin, A.; Montes de Correa, C. *Ind. Eng. Chem. Res.* **2009**, *48*, 2826–2835.
(28) Norskov, J. K.; Bligaard, T.; Rossmeisl, J.; Christensen, C. H. *Nat. Chem.* **2009**, *1*, 37.
(29) Christensen, C. H.; Norskov, J. K. *J. Chem. Phys.* **2008**, 128.
(30) Acevedo, O.; Jorgensen, W. L. *Acc. Chem. Res.* **2010**, *43*, 142.
(31) Hu, H.; Yang, W. T. *THEOCHEM* **2009**, *898*, 17.
(32) Moses, P. G.; Hinnemann, B.; Topsøe, H.; Nørskov, J. K. *J. Catal.* **2009**, *268*, 201.
(33) Kalita, B.; Deka, R. C. *J. Chem. Phys.* **2007**, 127.
(34) Efremenko, I.; Sheintuch, M. *J. Mol. Catal A: Chem.* **2000**, *160*, 445.
(35) Boyukata, M.; Belchior, J. C. *Croat. Chem. Acta* **2008**, *81*, 289.
(36) Roques, J.; Lacaze-Dufaure, C.; Mijoule, C. *J. Chem. Theory Comput.* **2007**, *3*, 878.
(37) Chen, L.; Zhou, C.; Wu, J.; Cheng, H. *Front. Phys. China* **2009**, *4*, 356.
(38) Moc, J.; Musaev, D. G.; Morokuma, K. *J. Phys. Chem. A* **2003**, *107*, 4929.
(39) Yanjin, W.; Zexing, C.; Qianer, Z. *Chem. Phys. Lett.* **2003**, *376*, 96.
(40) Meiyan, N.; Zeng, Z. *THEOCHEM* **2009**, *910*, 14.
(41) Barone, G.; Duca, D.; Ferrante, F.; La Manna, G. *Int. J. Quantum Chem.* **2010**, *110*, 558.
(42) German, E. D.; Efremenko, I.; Sheintuch, M. *J. Phys. Chem. A* **2001**, *105*, 11312.
(43) Efremenko, I.; Matatov-Meytal, U.; Sheintuch, M. *Isr. J. Chem.* **2006**, *46*, 1.
(44) Efremenko, I.; Sheintuch, M. *J. Catal.* **2003**, *214*, 53.
(45) D'Anna, V.; Duca, D.; Ferrante, F.; La Manna, G. *Phys. Chem. Chem. Phys.* **2009**, *11*, 4077.
(46) Mushrif, S. H.; Reya, A. D.; Peslherbe, G. H. *J. Mater. Chem.* **2010**, *20*, 10503.
(47) Prasomsri, T.; Shi, D.; Resasco, D. E. *Chem. Phys. Lett.* **2010**, *497*, 103.
(48) Sanz-Navarro, C. F.; Åstrand, P.; Chen, D.; Rønning, M.; van Duin, C. T.; Goddard, G. A. *J. Phys. Chem. C* **2010**, *114*, 3522.
(49) Bertani, V.; Cavallotti, C.; Masi, M.; Carra, S. *J. Mol. Catal A: Chem.* **2003**, *204*, 771.
(50) Bertani, V.; Cavallotti, C.; Masi, M.; Carra, S. *J. Phys. Chem. A* **2000**, *104*, 11390.
(51) Zanti, G.; Peeters, D. *Eur. J. Inorg. Chem.* **2009**, 3904.
(52) Bertin, V.; Agacino, E.; Lopez-Rendon, R.; Poulain, E. *THEOCHEM* **2006**, *769*, 243.
(53) Nava, P.; Sierka, M.; Ahlrichs, R. *Phys. Chem. Chem. Phys.* **2004**, *6*, 5338.
(54) Rochefort, A.; Fournier, R. *J. Phys. Chem.* **1996**, *100*, 13506.
(55) Valerio, G.; Toulhoat, H. *J. Phys. Chem. A* **1997**, *101*, 1969.
(56) Huber, B.; Hakkinen, H.; Landman, U.; Moseler, M. *Comput. Mater. Sci.* **2006**, *35*, 371.
(57) Mehmood, F.; Greeley, J.; Curtiss, L. A. *J. Phys. Chem. C* **2009**, *113*, 21789.
(58) Pallassana, V.; Neurock, M. *J. Catal.* **2002**, *209*, 289.
(59) Neurock, M. *Appl. Catal., A* **1997**, *160*, 169.
(60) Huang, Y. L.; Weng, C. M.; Hong, F. E. *Chem.—Eur. J.* **2008**, *14*, 4426.
(61) Piechaczyk, O.; Cantat, T.; Mezailles, N.; Le Floch, P. *J. Org. Chem.* **2007**, *72*, 4228.
(62) Sumimoto, M.; Iwane, N.; Takahama, T.; Sakaki, S. *J. Am. Chem. Soc.* **2004**, *126*, 10457.
(63) Chen, N.; Rioux, R. M.; Barbosa, L. A. M.; Ribeiro, F. H. *Langmuir* **2010**, *26*, 16615.
(64) Lu, G.; Lan, J.; Li, C.; Wang, W.; Wang, C. *J. Phys. Chem. B* **2006**, *110*, 24541.
(65) Avdeev, V. I.; Kovalchuk, V. I.; Zhidomirov, G. M.; d'Itri, J. L. *J. Struct. Chem.* **2007**, *48*, S171.
(66) Lim, D.-H.; Latoskie, C. M. *Environ. Sci. Technol.* **2009**, *43*, 5443 .
(67) Frisch, M. J.; Trucks, G. W.; Schlegel, H. B.; Scuseria, G. E.; Robb, M. A.; Cheeseman, J. R.; Montgomery, J. A., Jr.; Vreven, T.; Kudin, K. N.; Burant, J. C.; Millam, J. M.; Iyengar, S. S.; Tomasi, J.; Barone, V.; Mennucci, B.; Cossi, M.; Scalmani, G.; Rega, N.; Petersson, G. A.; Nakatsuji, H.; Hada, M.; Ehara, M.; Toyota, K.; Fukuda, R.; Hasegawa, J.; Ishida, M.; Nakajima, T.; Honda, Y.; Kitao, O.; Nakai, H.; Klene, M.; Li, X.; Knox, J. E.; Hratchian, H. P.; Cross, J. B.; Adamo, C.; Jaramillo, J.; Gomperts, R.; Stratmann, R. E.; Yazyev, O.; Austin, A. J.; Cammi, R.; Pomelli, C.; Ochterski, J. W.; Ayala, P. Y.; Morokuma, K.; Voth, G. A.; Salvador, P.; Dannenberg, J. J.; Zakrzewski, G.; Dapprich, S.; Daniels, A. D.; Strain, M. C.; Farkas, O.; Malick, D. K.; Rabuck, A. D.; Raghavachari, K.; Foresman, J. B.; Ortiz, J. V.; Cui, Q.; Baboul, A. G.; Clifford, S.; Cioslowski, J.; Stefanov, B. B.; Liu, G.; Liashenko, A.; Piskorz, P.; Komaromi, I.; Martin, R. L.; Fox, D. J.; Keith, T.; Al-Laham, M. A.; Peng, C. Y.; Nanayakkara, A.; Challacombe, M.; Gill, P. M. W.; Johnson, B.; Chen, W.; Wong, M. W.; Gonzalez, C.; Pople, J. A. *Gaussian 03*, revision E.01; Gaussian, Inc.: Wallingford, CT, 2004.
(68) Becke, A. D. *J. Chem. Phys.* **1993**, *98*, 5648.
(69) Lee, C. T.; Yang, W. T.; Parr, R. G. *Phys. Rev. B* **1988**, *37*, 785.
(70) Hay, P. J.; Wadt, W. R. *J. Chem. Phys.* **1985**, *82*, 270.
(71) Wadt, W. R.; Hay, P. J. *J. Chem. Phys.* **1985**, *82*, 284.
(72) Hay, P. J.; Wadt, W. R. *J. Chem. Phys.* **1985**, *82*, 299.
(73) Huang, S. Y.; Huang, C. D.; Chang, B. T.; Yeh, C. T. *J. Phys. Chem. B* **2006**, *110*, 21783.
(74) Yamauchi, M.; Ikeda, R.; Kitagawa, H.; Takata, M. *J. Phys. Chem. C* **2008**, *112*, 3294.
(75) Zuttel, A.; Nutzenadel, C.; Schmid, G.; Emmenegger, C.; Sudan, P.; Schlapbach, L. *Appl. Surf. Sci.* **2000**, *162*, 571.
(76) Zhou, Z.; Gao, F.; Goodman, D. W. *Surf. Sci.* **2010**, *604*, 131.

(77) Lee, S.; Kahng, S.; Kuk, Y. *Chem. Phys. Lett.* **2010**, *500*, 82.
(78) Solymosi, F.; Rasko, J. *J. Catal.* **1995**, *155*, 74.
(79) Wang, Y. N.; Marcos, J. A.; Simmons, G. W.; Klier, K. *J. Phys. Chem.* **1990**, *94*, 7597.
(80) Klivenyi, G.; Kovacs, I.; Solymosi, F. *Surf. Sci.* **1999**, *442*, 115.
(81) Henderson, M. A.; Mitchell, G. E.; White, J. M. *Surf. Sci.* **1987**, *184*, L325.
(82) Ramos, A. L. D.; Alves, P. D.; Aranda, D. A. G.; Schmal, M. *Appl. Catal., A* **2004**, *277*, 71.
(83) Fung, S. C.; Sinfelt, J. H. *J. Catal.* **1987**, *103*, 220.
(84) Lumbreras, E., Jr.; Sisler, E. M.; Shelby, Q. D. *J. Organomet. Chem.* **2010**, *695*, 201.
(85) Krylov, O. V.; Kiselev, V. F. *Adsorption and Catalysis on Transition Metal and Their Oxides*; Springer: Berlin, 1989.